Special Article

Gammaphotography

MALCOLM R. POWELL, M.D., *San Francisco*

■ *The Anger scintillation camera greatly broadens the range of studies performed by radioisotope imaging devices. Its ability to view in any direction, to make an image simultaneously of an entire field of view, and to obtain images rapidly, all serve to make scintiphotography analogous to fluoroscopy. Illustrations of its uses in static and dynamic gammaphotography and in numerical data processing are described.*

THE SCINTILLATION CAMERA developed by H. O. Anger at the Lawrence Radiation Laboratory and Donner Laboratory, University of California, Berkeley, is coming into sufficiently widespread use that this method of gamma radiation imaging deserves review.[1,3,4] The instrument produces a photographic image of sources of gamma radiation within its field of view. The image is formed continuously without motion of the instrument, so that stop-motion photographs or even motion pictures may be obtained. The image is referred to as a "scintiphoto" or "gammaphoto" and should be considered in some respects as similar to the more familiar radioisotope scan. Continuous imaging and the ability to obtain views rapidly while looking in any direction make the scintillation camera more analogous to a fluoroscope. The range of general clinical applications of the Anger scintillation camera as it is currently used in our laboratory is described herein.

The process of gamma-image formation by this instrument is simple in principle.[2] Gamma-rays are allowed to enter the detector only if parallel to the axis of parallel holes in the lead collimator. The gamma-rays are absorbed in a ½-inch thick, 12-inch diameter sodium iodide crystal. This converts the gamma ray energy to flashes of light at the points of absorption in the crystal. Since the crystal is relatively thin, the points of absorption are in nearly the same plane. An array of 19 photomultiplier tubes above the crystal are all exposed to the flashes of light or scintillations. The quantity of light photons "seen" by each photomultiplier tube is proportional to the distance of the tube from the scintillation. The photomultiplier tubes convert the light energy detected into greatly amplified electric pulses. The pulse sizes relative to the positions of the photomultiplier tubes are used, (to borrow a nautical term) to "take a fix" on the point at which the scintillation was detected in the crystal. This information is analyzed by a computer circuit and X and Y axis positioning signals are obtained. The process is similar to a vector analysis in electrocardiography. The positioning signals are used to produce a white dot on an oscilloscope viewing surface in the same relative position as the original radioactive disintegration. The oscilloscope is continuously photographed to accumulate sufficient numbers of these white dots to form an image. Figure 1 illustrates the major components of a camera system in the order described.

The field of view of the commercially available scintillation camera is round and of 10-inch diameter.* This size is usually sufficient to permit obtaining at a single view an image of both kidneys, or one lung or the liver. The system can analyze ten million events per minute. Because of

From the Nuclear Medicine Section, Department of Radiology, University of California School of Medicine, San Francisco.

Reprint requests to: Department of Radiology, University of California San Francisco Medical Center, San Francisco 94122.

*Pho-Gamma Scintillation Camera, manufactured by Nuclear-Chicago Corp., 333 East Howard Avenue, Des Plaines, Ill. 60018.

its physical characteristics, the resolution of the scintillation camera is best between gamma energies of 80 and 410 Kev, which include a wide range of clinically useful isotopes. Gamma spectroscopy allows the detection of one isotope in the presence of others. This permits use of several isotopes in one patient for sequential studies and also the differentiation of adjacent organs in single scintiphotos.

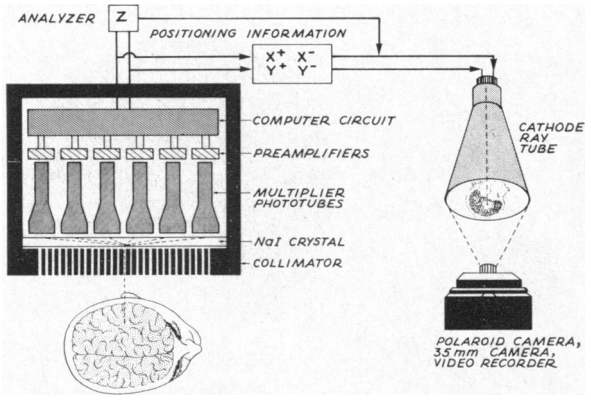

Figure 1.—Anger scintillation camera diagram. Detailed explanation of operation is given in the text. The system converts gamma-ray energy first to light energy and then to electric pulses. The pulses describe the position of origin of the original gamma-ray (X and Y pulses) and also its energy (Z pulse). The positioning information flashes the position of each event on an oscilloscope monitor only if the energy information is in the proper range, restricting the recorded image to gamma-rays of the selected energy range. The flashes of light that appear on the cathode-ray tube are collected photographically by timed exposure to form an image of the distribution of radioactivity in the subject.

As a means of further definition of the characteristics of this instrument, Table 1 provides comparison with a conventional rectilinear radioisotope scanner. It should be understood that the more familiar scanner produces a best resolved image at a depth near the focal point of its collimator. The Anger scintillation camera instead produces an image of the distribution of a selected radiation energy within its field of view, subject only to decrease by internal radiation absorption within the patient. The internal absorption results in less efficient imaging of deep parts than of those close to the detector surface. This impaired efficiency increases noticeably at lower gamma-ray energies. Figure 2 shows this effect in a commercially available liver phantom.*

The scintillation camera was the first commercial instrument generally available for gamma-imaging that produced an image smaller than the original labeled organ. Several other gamma-imaging instruments now also produce minified images. To the uninitiated viewer, these small images present some hurdles in visual psychology. Actually, more data points are produced in most of these minified images than in the previously accepted norm, the 1:1 sized rectilinear scan. Furthermore, the minimum resolution obtained with the gamma-imaging procedures in general use is between ½ inch and 1 inch, although better resolution is ob-

*Available from Alderson Research Laboratories, Inc., 48-14 33rd Street, Long Island 1, New York.

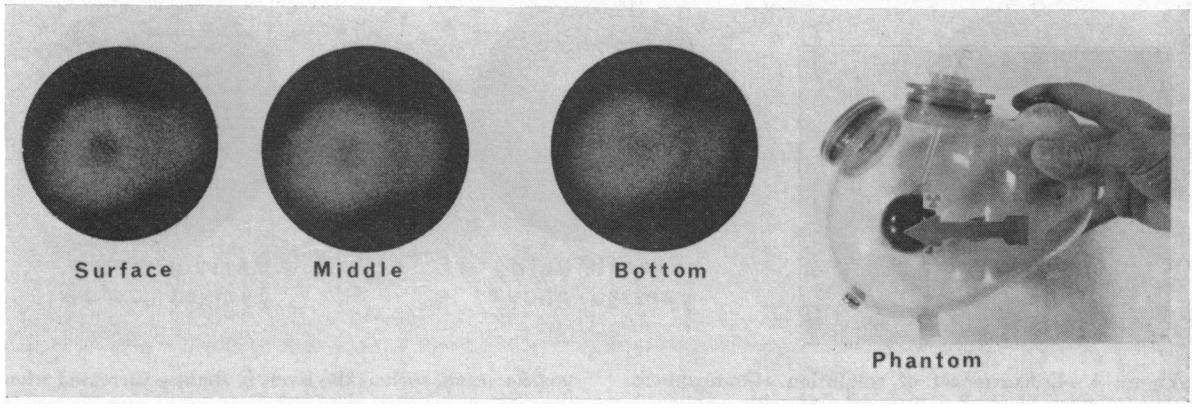

Figure 2.—Phantom studies. The plastic liver phantom was filled with a solution containing technetium 99m pertechnetate. The 1½-inch dark colored sphere contains no radioactivity. It is positioned by means of the long plastic dowel that holds it within the phantom. The gammaphoto at the left was obtained with the sphere at the surface of the phantom, the next with the sphere centered in the phantom, and the last with it at the bottom of the phantom, farthest from the camera. The depth of the phantom at this point is 4¾ inches. The phantom was photographed while under 2 inches of water, to simulate the situation of the liver *in vivo*. These photographs illustrate that surface defects are visualized more readily with the scintillation camera than are defects at a distance from the camera that are below a considerable amount of radioactive label. Because of the speed of the scintillation camera, multiple scintiphotos are obtained easily. When a large organ is studied, such as the liver, effort is made to photograph the organ from all directions, so as to optimize the probability of seeing abnormal labeling.

tainable in many studies. The most efficient image for recognition of this magnitude of resolution at usual viewing distances is about the size of the minified images. Morgan[10] and Tuddenham[13] both have discussed this point with regard to diminishing lenses for roentgenogram interpretation. Their data indicated that the most efficient viewing distance for the resolution available in conventional scans is of the order of 5 meters. Figure 3 shows the effect of image size upon spatial resolution. The effect can also be observed readily by stepping back farther while viewing the large picture. Defocusing increases apparent resolution, as is also illustrated in Figure 3, and may be duplicated by squinting while looking at a scintiphoto or by removal of eye-glasses.

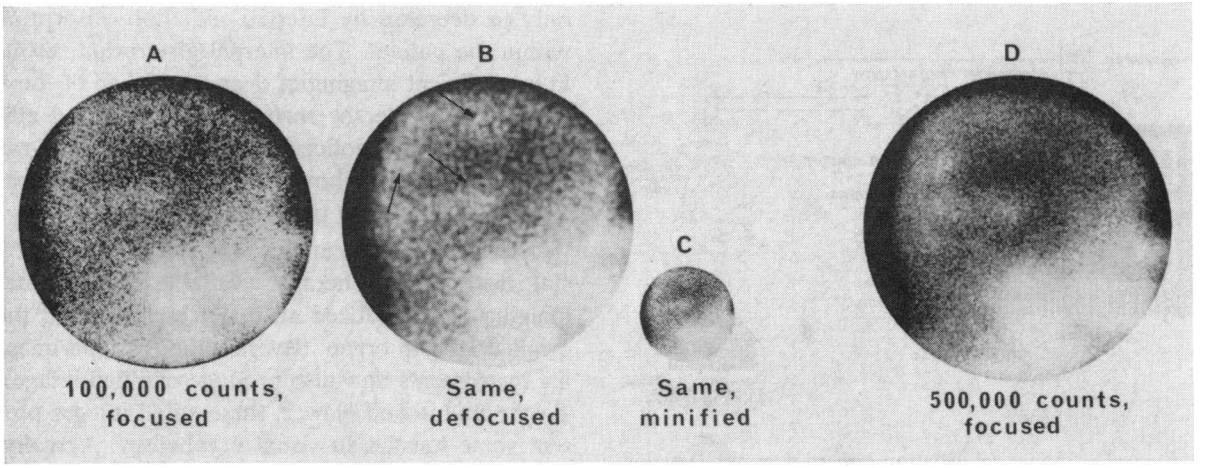

Figure 3.—Image contrast enhancement. (A) A right lateral view of the head with 100,000 dots collected in a 34-second exposure. The photograph is reproduced as originally obtained. (B) The same photograph reproduced with the dots "defocused." This increases ease of recognition of some image details. Several areas of abnormality of capillary permeability are present. (C) The original photograph reproduced in a minified image size also increases ease of recognition of details. (D) An image of the same subject obtained by collecting 5 times as many counts in a 173-second exposure. A decreased dot intensity was used in the cathode-ray tube display so as to avoid overexposure of the photographic film. This image also shows increase of contrast between target and nontarget areas and improved resolution. Arrows identify several of the definite abnormalities.

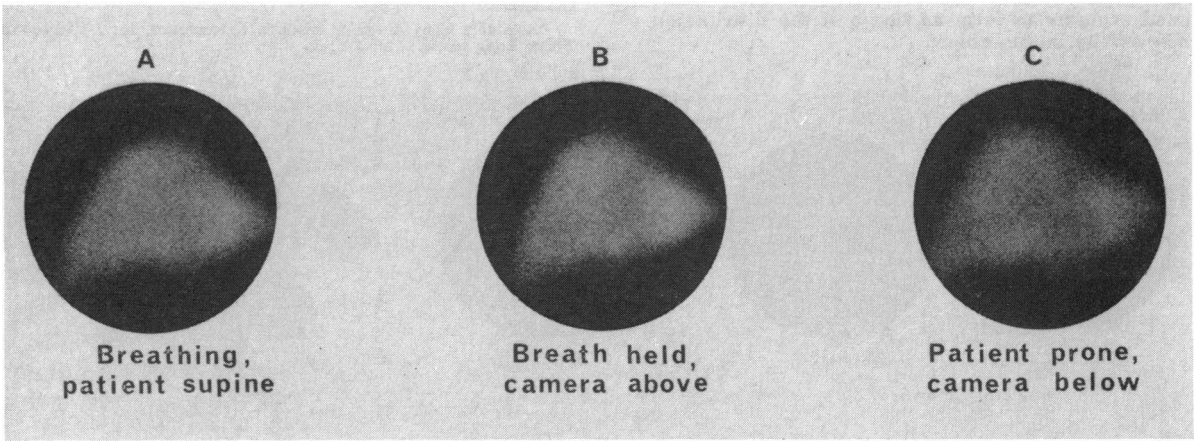

Figure 4.—Enhancement of resolution. Gammaphotos in the anterior view of a liver labeled with technetium 99m colloid demonstrate the effect of changes in camera-target orientation. (A) and (B) were obtained with the camera detector directed down at a supine patient and (C) with the detector directed up at a prone patient. Save for the change in detector-patient orientation, these anterior views of the liver are the same. During (A) the patient was breathing normally, but during (B), data were obtained only while the patient had paused in normal respiration, each pause being in relatively the same position. These gammaphotos illustrate that resolution of a mobile organ, such as the liver, is slightly increased when the photographs are obtained during cessation of respiration. Also resolution increases when this large organ is brought closer to the camera detector surface by means of placing the patient face-down with the viewing surface of the detector against the abdomen. (C) A central decrease of labeling within the liver image probably corresponds to the porta hepatis and to the large volume of venous blood in this area that is unlabeled. Minor irregularities of labeling throughout this liver image are greater than seen usually in a normal liver and may reflect some hepatocellular disease.

Clinical Scintiphotography

The principal clinical uses of the scintillation camera in our laboratory fall into three general categories: static scintiphotography, dynamic scintiphotography, and numerical data detector and processor. The organs or tissues routinely studied by scintiphotography now include the brain, thyroid and parathyroid glands, lungs, liver, spleen, bone marrow, pancreas, kidneys, joints, placenta, heart and great vessels.

Static gammaphotography is not an entirely accurate description, since many of the so-called static techniques may involve photographic exposure only when the patient is motionless. Respira-

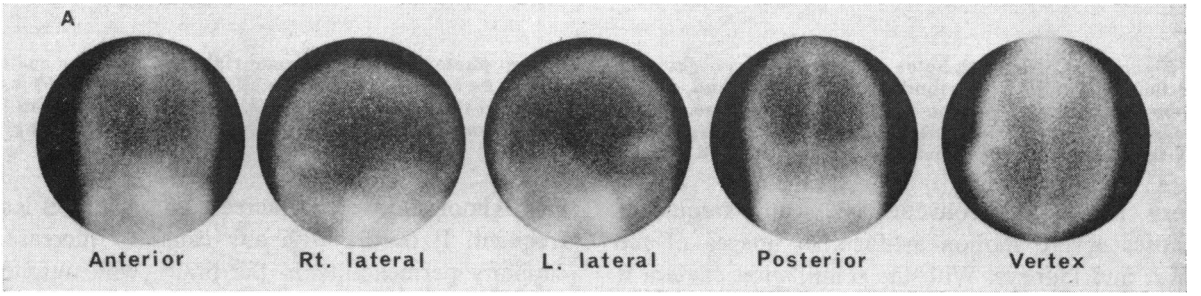

Figure 5.—Typical normal multiple view gammaphotograph studies. (A) This series of gammaphotos of a normal brain was obtained by injecting 12 millicuries of technetium 99m pertechnetate intravenously. A constant exposure time of 210 seconds was used so that all photographs would be comparable. Approximately 500,000 counts comprise a picture. Labeling in the brain areas is less than in the vascular areas since the pertechnetate does not readily pass the blood brain barrier. The superior sagittal sinus is recognized easily in the midline of the anterior, posterior, and vertex views where the camera is directed down at the top of the patient's head. For the vertex view a shield is placed over the shoulders so that the rest of the patient's body does not show in the gammaphoto. The transverse sinuses are seen joining the torcular in the posterior view and appear as bright horizontal areas of labeling posteriorly in either lateral view. Bright labeling of the salivary glands is recognizable below the brain areas.

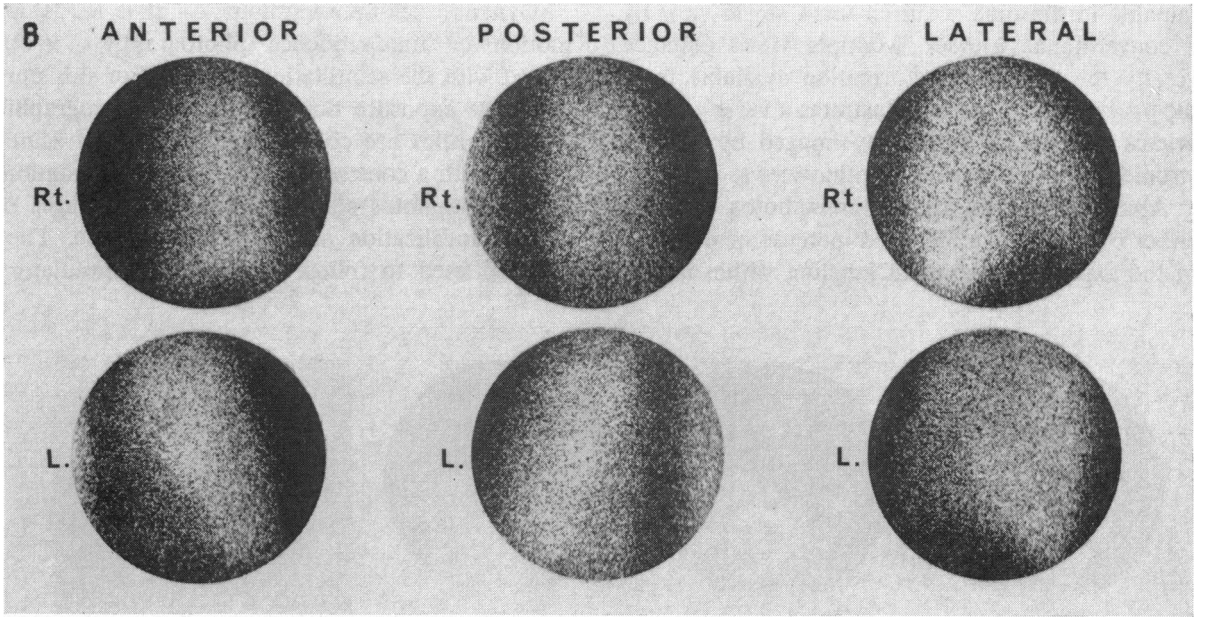

Figure 5(B).—A series of lung gammaphotos obtained again with a constant exposure time of 190 seconds to obtain approximately 80,000 counts per picture. The label is I-131 labeled macroaggregated human serum albumin which lodges temporarily in the microvasculature of the lungs and provides an opportunity to photograph the distribution of pulmonary blood flow. These lungs show fairly uniform labeling in all views, although some minor irregularities are present that are not entirely normal. This series of gammaphotos shows the degree to which pulmonary blood supply has been reestablished three months after extensive thromboembolism (note Figure 6, C). The unlabeled mediastinum and heart images are seen centrally with the outlines of the lung recognizable to either side. Because of the limited field size of the scintillation camera, each lung is photographed separately.

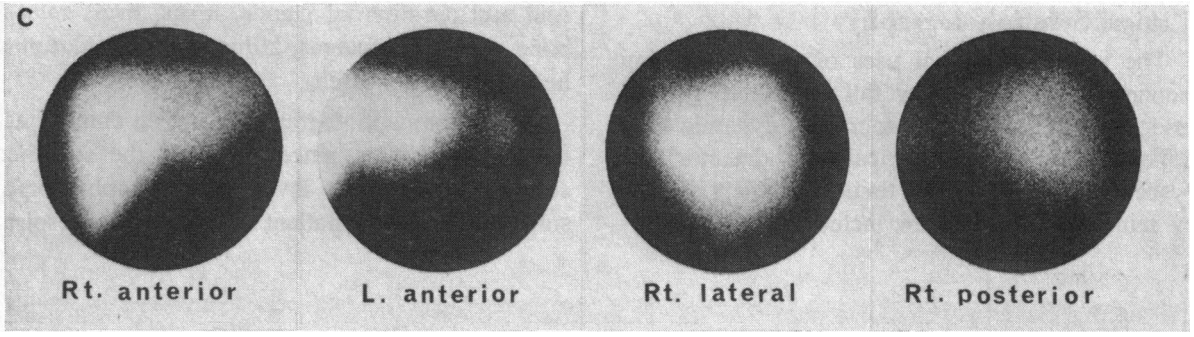

Figure 5(C).—Scintiphotos of normal liver showing technetium colloid distribution in the liver and spleen immediately after injection of a 3.5 millicurie dose. Again, exposure time was constant at 180 seconds in all pictures of this series. Approximately 500,000 counts were imaged in each photograph. The normal right and left lobe anatomy can be recognized and a small spleen is visualized just lateral to the left lobe of the liver. Because the spleen is a posterior organ, this anterior view does not show it well.

tory motion in conventional scans frequently causes severe motion artifacts in images of the liver and kidneys. With the scintillation camera it is possible to obtain stop-motion photographs without motion artifacts, thereby improving resolution[8] (Figure 4).

Static scintiphotos are obtained with the detector viewing the patient from as many directions as possible. As has been explained, the scintillation camera shows best resolution for the portion of the target nearest the detector. With the great sensitivity of the camera, several views are obtainable in the time required for a single view by a conventional scanner. Multiple views enhance greatly the diagnostic information available from the procedure.[7] Figure 5 illustrates a variety of the organs and tissues commonly imaged by this instrument and the various routine views.

Abnormalities in static gammaphotos are seen either by virtue of a localized increase or decrease of the expected amount of labeling within an organ. Abnormality as an increase of labeling is less frequent. It occurs with any cause of increased capillary permeability in the brain, with autonomous thyroid adenomas, in arthritic joints, and in direct labeling of malignant lesions as accomplished by Cavalieri and coworkers[6] with ^{75}Se selenite. More often, scintiphoto abnormalities are seen as decreased labeling in a labeled lung, liver, spleen, kidney, pancreas or thyroid gland. Figure 6 illustrates some typical abnormal static scintiphotos with both types of abnormalities represented.

Dynamic scintiphotography — that is, "stop-motion" or "time sequence" photography — is obtained with the scintillation camera. For this purpose, the exposure times and other photographic characteristics are constant for a series of scintiphotos with a constant camera-patient orientation. Such scintiphotos allow evaluation of changes of isotope localization as a function of time. They may be used to follow labels in the circulatory

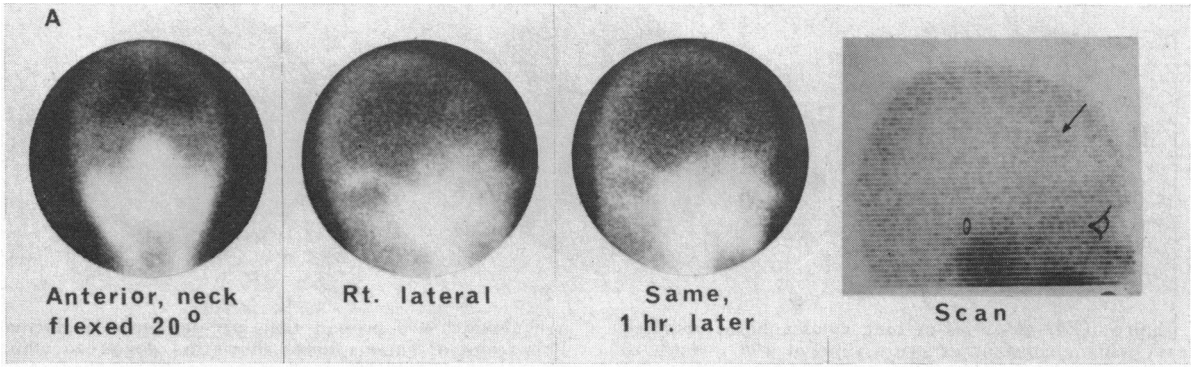

Figure 6.—Abnormal static gammaphotograph studies. (A) Abnormality of capillary permeability of brain (arrow) shown here is considered to be the result of arterial sclerotic cerebrovascular disease. A conventional rectilinear scan using a fine focus collimator positioned for the known depth of the abnormality provides for comparison of the gammaphotographs with the more generally understood scanning technique. The abnormality is just visible in the scan.

system, in the airways, during renal excretion, during secretion of dye by the liver, and in many other processes.[5,9,11,12]

The amounts and the volumes of labeled pharmaceuticals are physiologic. Therefore, the data provided by dynamic scintiphotography tend to be physiologic as opposed to those with nonphysiologic doses of radiopaque dyes and a variety of conventional roentgenographic procedures. Figure 7 illustrates some abnormal dynamic scintiphoto studies.

The interest in dynamic scintiphotography has been paralleled by that in the scintillation camera system as a numerical data detector and processor. The commercially available scintillation camera is equipped with a built-in simple data processor. Operation with an electronically divided field of view allows separation of counts from each kidney or from each cerebral hemisphere. The data may be further processed by operation in a preset time mode with automatic cycling so that data are counted from each half of the field of view for the

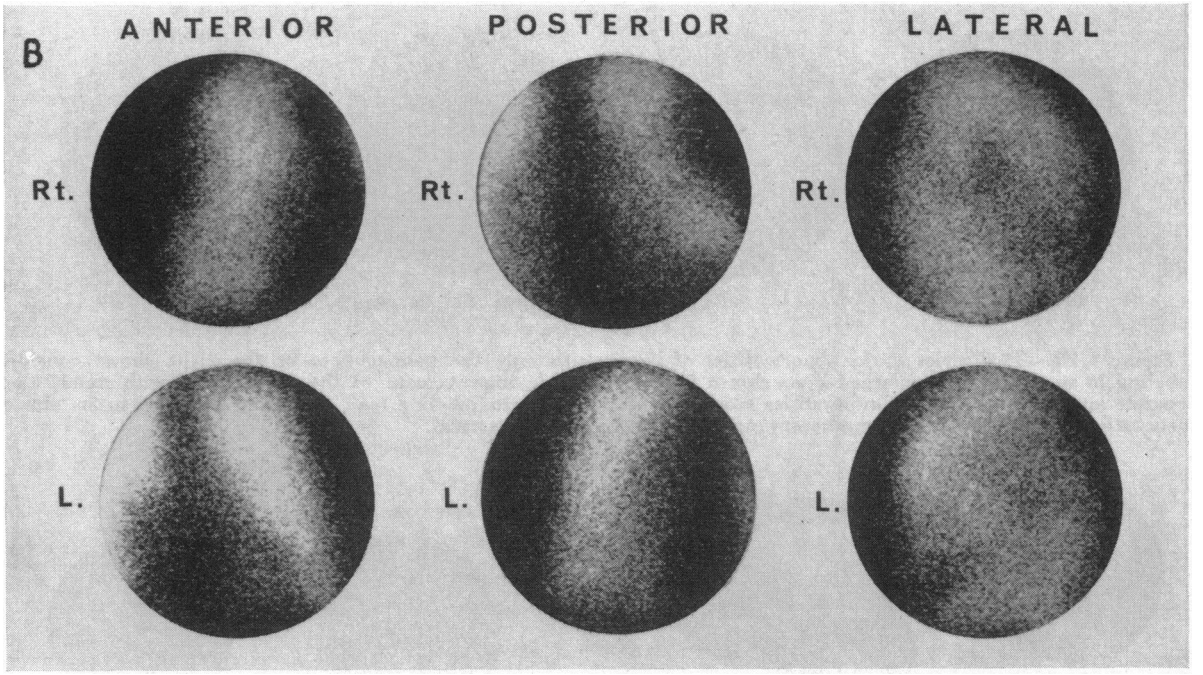

Figure 6(B).—Focal abnormalities of patterns of pulmonary arterial perfusion are seen in several areas in these lungs. These abnormalities are caused by thromboembolism, but similar defects of perfusion might be seen when the lung is displaced by tumor or blebs, or when pulmonary arterial perfusion is decreased by other causes, notably bronchogenic carcinoma, congenital anomalies, and involvement in pulmonary fibrosis.

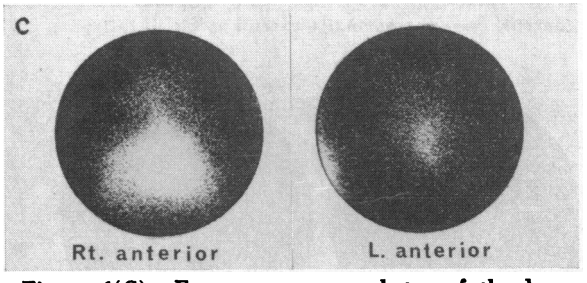

Figure 6(C).—Emergency gammaphotos of the lungs were obtained with I-131 labeled macroaggregated albumin. The result of massive pulmonary thromboembolism is illustrated. This patient was too ill to undergo further views. The exposure time for each of these views was 231 seconds. Because of the positioning mobility of the detector, these studies can be obtained in a sitting position. These grossly abnormal gammaphotos eventually showed clearing, with nearly normal scintiphotos (Figure 5, B) resulting three months after these emergency gammaphotos.

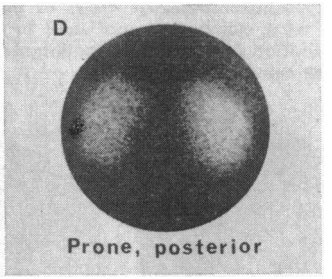

Figure 6(D).—A posterior view gammaphoto of Hg-203 chlormerodrin-labeling of kidneys. The left kidney appears somewhat smaller and less well labeled than the right. Significant hypertension is present in this patient and the left kidney is known to be involved with fibromuscular hyperplasia causing renal ischemia. The right kidney is imaged somewhat lower in position than is usual with the patient prone, owing to surgical fixation two years previously for fibromuscular hyperplasia of the right renal artery. This gammaphoto required 900 seconds and there are 39,000 counts in the right half of the field of view and 28,000 in the left half, a measure of the discrepancy in the amount of labeling in either kidney.

preset time interval, printed on paper tape at an extremely rapid rate (30 lines per second), and the process recycled. Figure 8 (A) shows a hippurate renogram obtained in this manner. A further refinement, but similar in principle, would be the ability to specify electronically that numerical data would be obtained from a defined area of the field of view—for example, from just the area representing one kidney. This is in essence what may be done with digital data processing. Such numerical processing allows compensation to make response uniform from all areas of the detector, subtraction of data (one organ image by one label from this organ's image, plus a second organ by a second label to show only the second organ), extraction of area counts per unit time, and many other maneuvers. Figure 8 (B) shows scintillation camera data in a multichannel analyzer display.

The strength of analyzer-processed data lies in the speed and convenience of processing digital

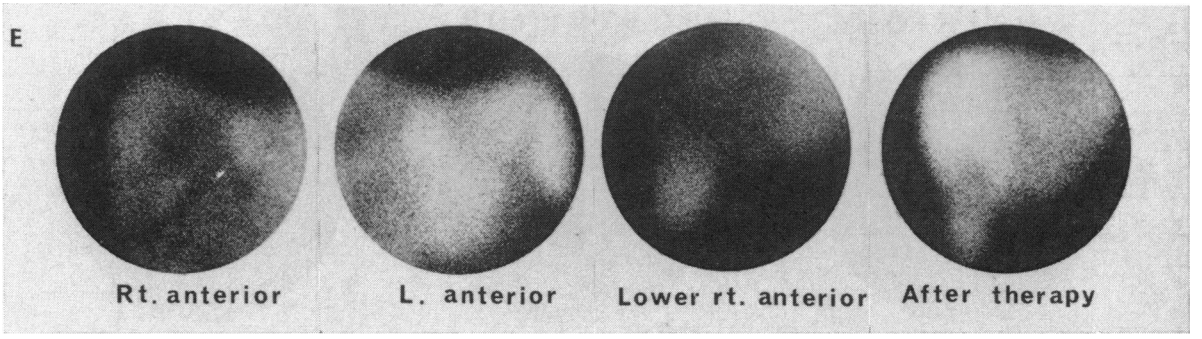

Figure 6(E).—This series shows abnormalities of liver labeling in an enormously enlarged liver, shown in three separate anterior views. The abnormalities resulted from metastatic seminoma. After chemotherapy and radiation therapy the gammaphoto at the right shows considerable improvement of the liver image with much more uniform labeling, and a marked decrease in its size to nearly normal.

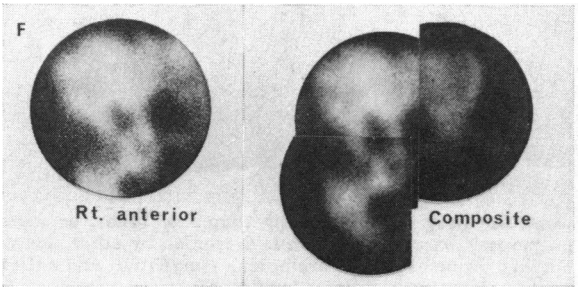

Figure 6(F).—These anterior views of polycystic liver disease show what can be accomplished by composite of several gammaphotos when a grossly enlarged organ does not fit into one camera field of view.

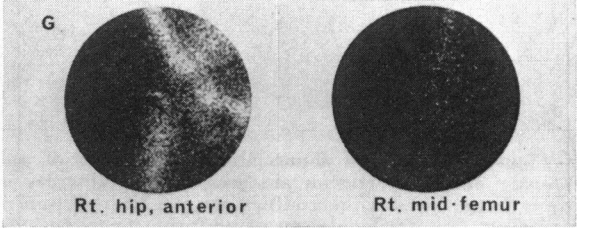

Figure 6(G).—Gammaphotos of the pelvis show increase of marrow labeling and extension of marrow into the right mid-femur, consistent with marrow hypertrophy. Marrow does not normally extend as far distally.

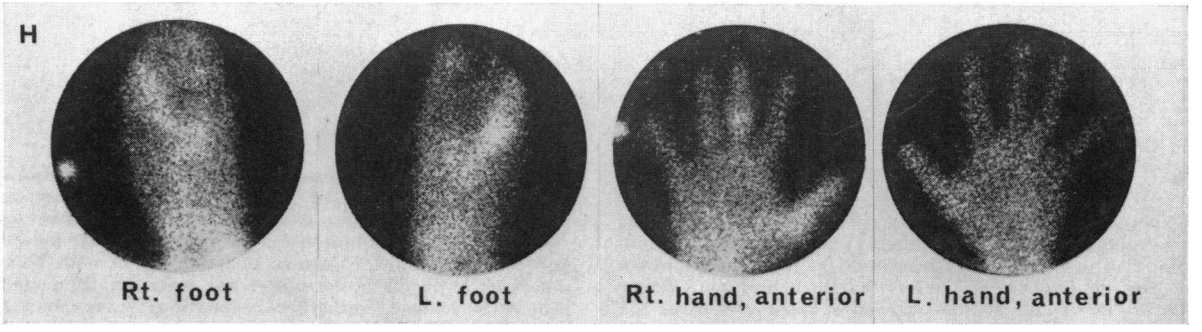

Figure 6(H).—These gammaphotos were obtained shortly after injection of 10 millicuries of technetium pertechnetate and show arthritic involvement of peripheral joints. A striking symmetric involvement of the fourth phalangeal-metatarsal joints is seen and increased labeling is distributed with less symmetry in other joints. The right third proximal interphalangeal joint of the hand and the right first metacarpophalangeal joint are the only ones involved in the two-hand gammaphotos. This patient had rheumatoid arthritis.

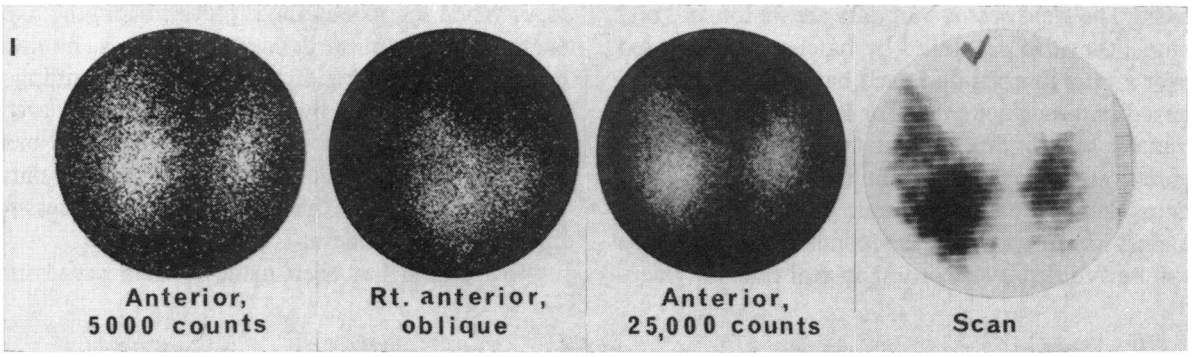

Figure 6(I).—Gammaphotos of the thyroid and a conventional thyroid scan are compared. In these gammaphotos the thyroid was relatively enlarged compared with the sizes of the images in the other gammaphotos, because a different collimator was used. This single pinhole collimator produces the relatively larger images when the pinhole is close to the target and relatively smaller when it is farther away. By obtaining pictures with the pinhole close to the thyroid, the whole field of view is filled by the image. In the 5,000-count anterior and right anterior oblique views, the gammaphotos show increased labeling in the lower pole of the right thyroid lobe. Just above and lateral to this area is one of decreased labeling, better seen in the anterior oblique than in the anterior view. The 25,000-count anterior view defines the distribution of radioiodide somewhat better than did the previous picture. The scan also shows essentially the same findings with better labeling by radioiodide of the lower pole of the right lobe than elsewhere. A cold nodule above and lateral to this area of relatively greater uptake is poorly defined.

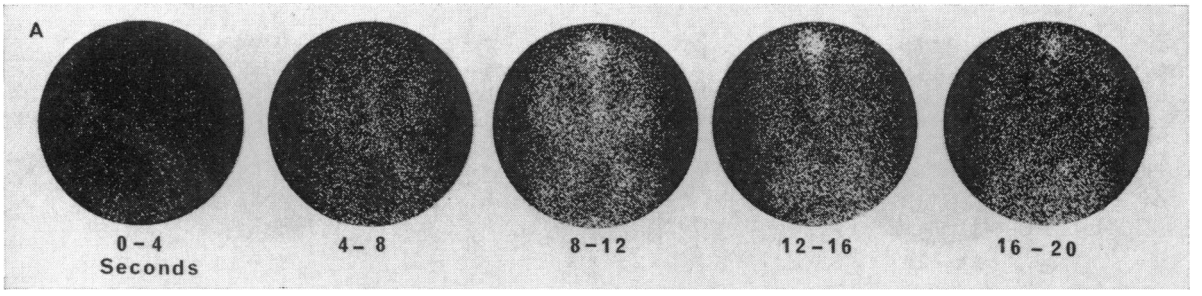

Figure 7. — Dynamic gammaphotograph studies. (A) This sequence of 4-second exposures was obtained after peripheral intravenous injection of 12 millicuries of technetium 99m pertechnetate. The camera images an anterior view of the patient's head. In the 4-second and the 8-second gammaphotos are seen patterns of the carotid artery, middle cerebral arteries, and anterior cerebral arteries plus the midline vasculature. Labeling of the right carotid artery pattern is less than of the left, indicating that the flow through this vessel is less. In the 12-second scintiphoto, bright labeling is seen of the superior sagittal sinus and also of the midline vascular structures. Thereafter, the image of the superior sagittal sinus fades away. No abnormal labeling is seen within areas of the brain hemispheres to suggest any sort of a vascular abnormality.

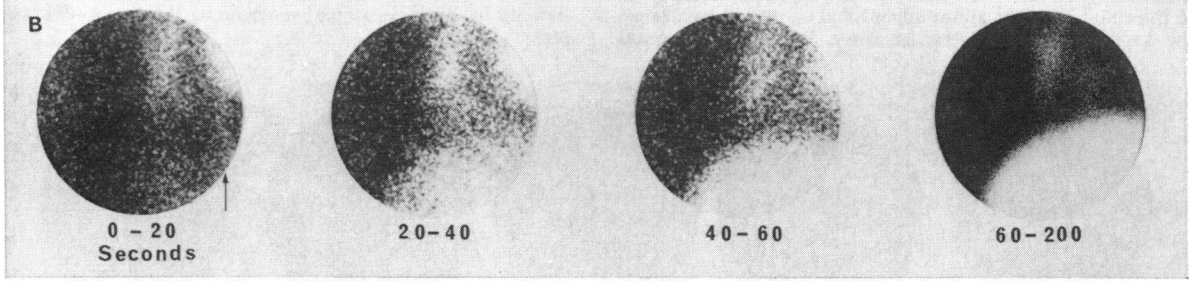

Figure 7(B).—This series of scintiphotos shows an interesting and as yet undescribed technique for demonstrating pleural and pericardial effusion. The patient is studied in the upright position with the camera visualizing the heart and the right hemidiaphragmatic areas. An injection of technetium 99m colloid is given and a series of 20-second scintiphotos is obtained, using bright dots. These show in the first 20 seconds the labeling of the right heart chambers and the pulmonary blood flow in the base of the right lung. A faint image of the abdominal aorta is seen below the heart. The next gammaphoto in exactly the same position shows a marked increase in labeling in the liver area with some decrease in the lung and heart areas. In the third photo between 40 and 60 seconds, the liver labeling has progressed. The distance between the right ventricle and the liver and the right ventricle and the lung is somewhat increased over normal and is consistent with the effusions in the pericardium and the pleural space. The diagnosis here was widely metastatic seminoma. A late gammaphoto using accumulation of a much greater number of dots over a prolonged exposure with diminished dot intensity shows in the same position a residual labeling of the base of the right lung and the labeling within the liver.

data. The weakness is that data are no longer "real time"; they are processed by batches accumulated over a time interval and each batch must be transferred onto magnetic tape for later processing. The transfer of a buffer content (that is, a batch) requires appreciable dead time, limiting the minimum time period for dynamic data acquisition by a single buffer to 1 or 2 seconds. This limitation can be avoided by recording in real time on videotape. When the video tape is played back, the light energy flux from a defined area of a monitor oscilloscope may be detected by photomultiplier tube and recorded by strip chart. Other areas similarly recorded are all on the same time base and may be compared as parallel analog data. Figure 8 (C) shows this variety of data processing by scintillation camera.

No mention has been made of data processing

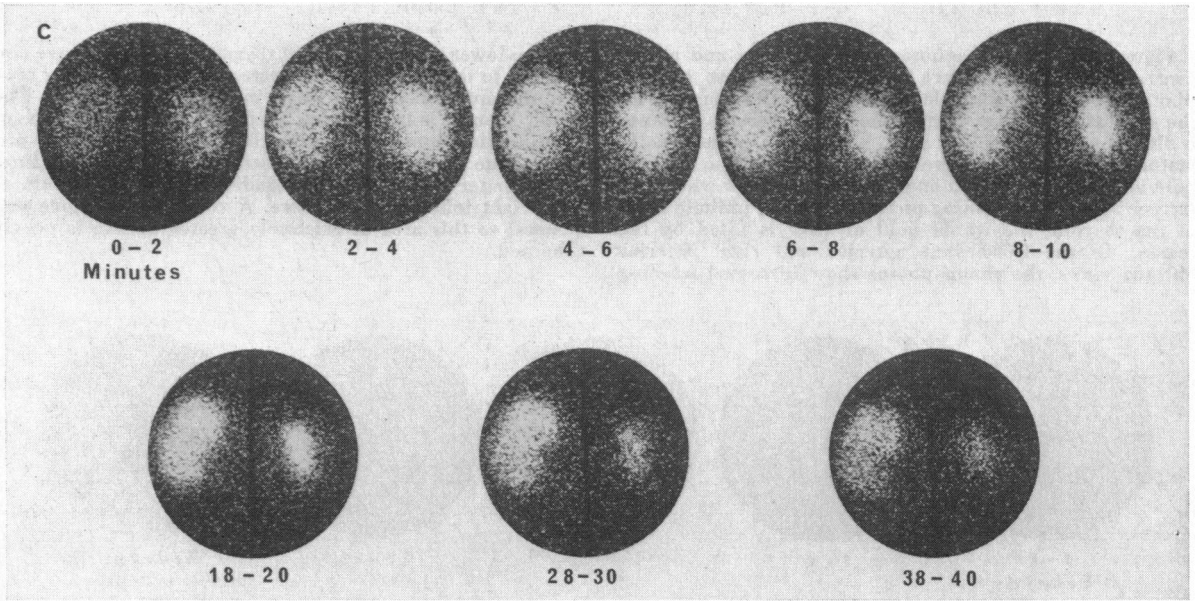

Figure 7(C). — A posterior view gammaphoto of the same patient of Figure 6, D. I-131 hippurate was injected and a series of scintiphotos was obtained in exactly the same position as the previously illustrated Hg-203 chlormerodrin picture. The right kidney is seen to accumulate the hippurate rapidly and drain the hippurate into its central or pelvic area. The label is then lost from the field of view of the camera because of drainage into the ureter and the bladder. The left kidney is seen to accumulate the hippurate at a slow rate and also to retain the label within the renal image to times when label should have cleared the kidney. The label, furthermore, is out in the renal cortex on the left and there is no evidence of an obstructive process involving the left renal pelvis. The reason for the delay of the excretion of the hippurate is an increased water resorption and a decrease of urine volume. This causes the late apparent "hyperconcentration," commented upon in various pyelographic studies, and is similar to the abnormalities defined in renovascular hypertension by the Stamie-Howard test. The advantage of gammaphotography is its ability to define regional renal function as opposed to function of an entire kidney, as would be defined by a radioisotope renogram or the Stamie-Howard test.

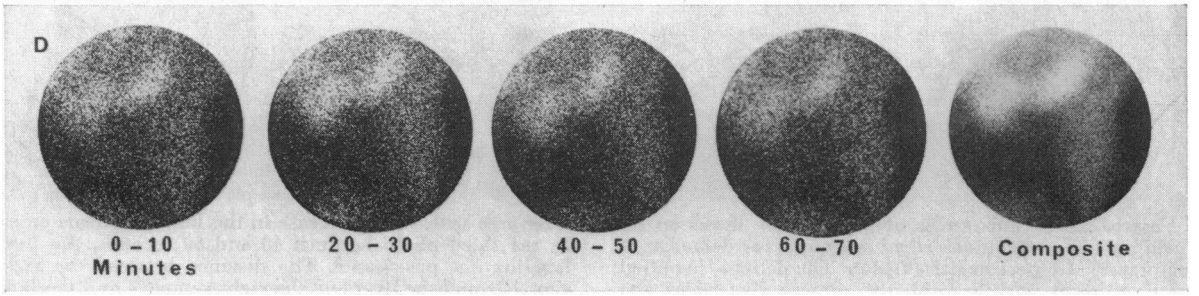

Figure 7(D). — This series illustrates pancreatic labeling by utilization of ^{75}Se methionine for resynthesis of pancreatic enzymes after pancreatic exocrine secretory function has depleted these enzymes. Illustrated is a perfectly normal pancreas with the head and tail well defined and separated by a defect caused by the impression of the abdominal aorta across the posterior surface of the pancreas. Changing amounts of labeling often can be seen in such a series of scintiphotos as enzymes are synthesized and secreted. The last picture is a photographic composite of eight preceding exposures, showing approximately 500,000 counts in one pancreatic scintiphoto. The abdominal musculature is seen in the left flank and labeling is seen above the pancreatic image where uptake has occurred in the liver.

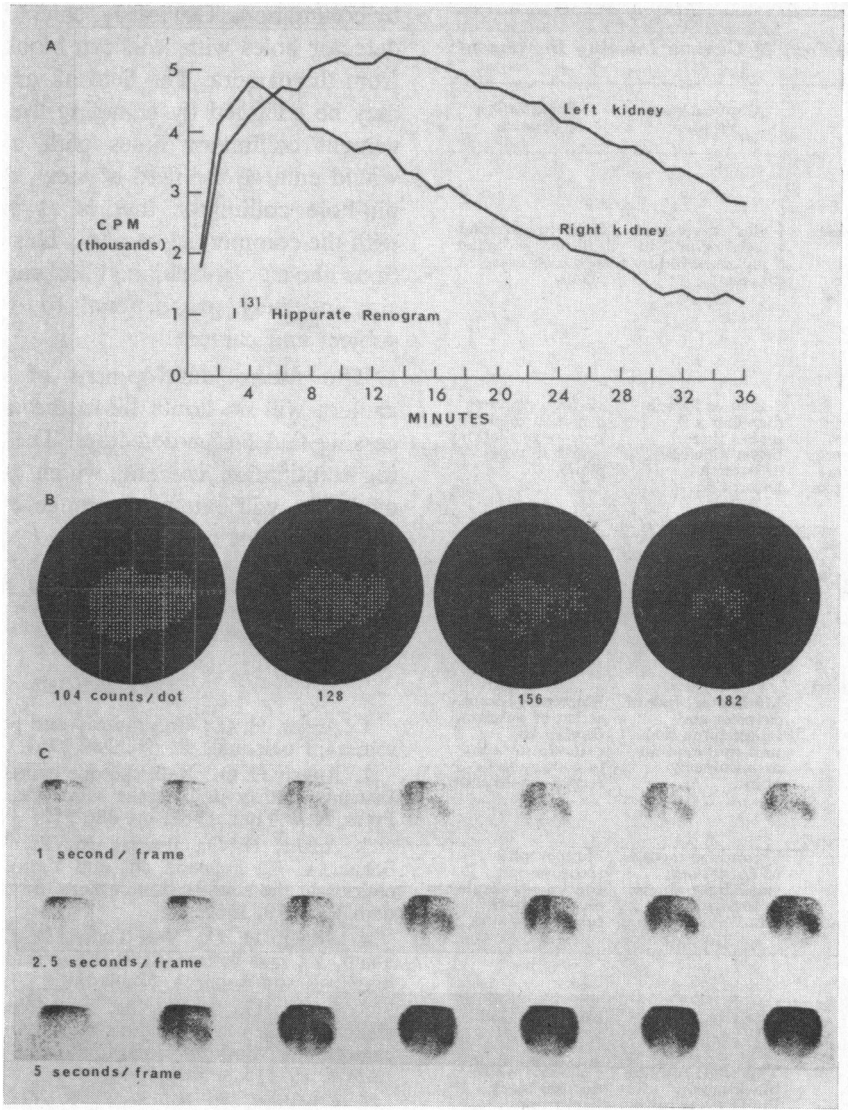

Figure 8.—Scintillation camera data processing. (A) This hippurate renogram was obtained with the scintillation camera by plotting numerical data recorded by a rapid printer from each half of the camera field of view. The count-rate over the right kidney follows a normal course with rapid accumulation of counts in the first four minutes because of labeling of the renovascular blood pool and then by tubular function with concentration of the hippurate in the renal tubules. Following this the count-rate peaks at four minutes and the drainage phase is normal for this type of renogram and patient position. The left kidney tracing is abnormal with a slower accumulation of counts, a broad delayed peak, and retention of counts in the kidney. This sort of curve could be reproduced by obstruction to ureteral drainage, but this is the renogram obtained simultaneously with the scintiphotos in Figure 7 (C) and these demonstrated that the retained counts are in the renal cortex. Drainage from the left renal pelvis was not delayed, as would occur with obstruction. Therefore, this renogram represents a prolongation of hippurate transit time, the result of increased water resorption in the cortex, and is consistent with the diagnosis of renovascular hypertension. (B) Static gamma-photos showing data-processing by a multichannel analyzer. A 4096-channel analyzer* was used to display the number of counts per area in a 64 x 64 array of analyzer positions. If a dot is illuminated, it indicates a given number of counts per area at that position. The number of counts represented per dot is labeled in the illustrations. The image shown is the liver phantom illustrated in Figure 2. As the analyzer is adjusted to show increasing numbers of counts per channel, the defect caused by the dark-colored sphere in the center of the phantom becomes visible. This analyzer data manipulation is what might be referred to as "electronic dissection of gamma anatomy." (C) Gammaphotos of renal blood flow with technetium 99m pertechnetate injected into a peripheral vein. The data from the scintillation camera were recorded first by video tape. The video tape was played back and 35 mm photographs were obtained at a rate of one per second, one per 2.5 seconds, and one per five seconds, showing the effect of changes in exposure time on image density in these dynamic studies. The blood-flow pattern in these kidneys was normal.

*Nuclear Data Inc., 100 West Golf Road, Palatine, Ill. 60067.

TABLE 1.—*Comparison of Gamma Imaging Instruments*

Function	*Conventional Scanner*	*Scintillation Camera*
Collimation		
Holes in lead absorber; gamma-rays from selected angles pass through holes; other gamma-rays absorbed in lead.	Holes converge to a focal point 3 to 5 inches beyond detector.	Holes are parallel and perpendicular to the detector plane.
Energy Conversion		
Crystal: NaI with thallium seeding absorbs gamma-rays, converts gamma energy to light (scintillation) at points of absorption.	3-inch or 5-inch diameter x 2 inches thick: better efficiency of gamma absorption	12-inch diameter x ½ inch thick: keeps scintillations nearly in same plane.
Multiplier phototubes detect light energy, convert and amplify as electrical pulse.	One	Nineteen, in an array to "take a fix" on each scintillation
Image Formation		
Information positioned in image by	Mechanical link of detector and image formation unit to record an area point by point.	Electronic computation of position, display on cathode-ray tube to continuously record whole area.
Gamma image recorded by	To and fro motion of dot tapper; small light source to expose x-ray film.	Photographic recording of continuous display on cathode-ray tube.
Result		
Image size	Life size, 1:1.	Miniature, 1:8.
Image type	Tap scan: rows of black taps. Photo scan: rows of grey to black film exposures.	Polaroid: white dots on black background. Conventional film: black dots on clear background.
Data density in image (compared with time for image formation).	Low	High
Speed	Low—used primarily for static studies.	High—sufficient for dynamic studies, e.g., blood-flow imaging.
Miscellaneous		
Field of view	To 14x17 inches, rectangular.	10 inches, circular.
Direction of view	Usually down; up in a few models.	Any
Useful energy range	25 to 520 Kev.	80 to 410 Kev (can be extended to 510 Kev by special collimation).

by collimation. Obviously, shielding of part of the detector holes with lead can block unwanted data from the camera. The field of view of the camera may be enlarged by changing the collimation; divergent collimator holes with a negative focus would enlarge the field of view, as will the single pin-hole collimator that is at present available with the commercial camera. This collimator functions like an old-fashioned box camera, with image size inversely proportional to distance between subject and camera.

The future development of the scintillation camera will no doubt lie in the area of data processing and larger detectors. The positron detecting scintillation camera, which is now becoming available, will extend the range of isotopes which the instrument can image.

ACKNOWLEDGMENT: The capable assistance of Mrs. Laurel Schaubert in the preparation of illustrations is gratefully acknowledged.

REFERENCES

1. Anger, H. O.: Gamma-ray and positron scintillation camera, Nucleonics, 21:56, Oct. 1963.

2. Anger, H. O.: Radioisotope cameras, *in* Hine, G. J.: Instrumentation in Nuclear Medicine, Vol. 1, Academic Press, New York, 1967, pp. 486-552.

3. Anger, H. O., Powell, M. R., Van Dyke, D. C., Schaer, L. R., Fawwaz, R., and Yano, Y.: Recent applications of the scintillation camera, Strahlentherapie (Sonderb.), 65:70, 1967.

4. Anger, H. O., Van Dyke, D. C., Gottschalk, A., Yano, Y., and Schaer, L. R.: The scintillation camera in diagnosis and research, Nucleonics, 23:57, Jan. 1965.

5. Burke, G., Halko, A., and Coe, F. L.: Dynamic clinical studies with radioisotopes and the scintillation camera. I. Sodium iodohippurate I-131 renography, JAMA, 197:15, 4 July 1966.

6. Cavalieri, R. R., Scott, K. G., and Sairenji, E.: Selenite (^{75}Se) as a tumor-localizing agent in man, J. Nucl. Med., 7:197, Mar. 1966.

7. Gottschalk, A.: Radioisotope scintiphotography with technetium 99m and the gamma scintillation camera, Amer. J. Roentgen., 97:860, Aug. 1966.

8. Gottschalk, A., Harper, P. V., Jiminez, F. F., and Petasnick, J. P.: Quantification of the respiratory motion artifact in radioisotope scanning with the rectilinear focused collimator scanner and the gamma scintillation camera, J. Nucl. Med., 7:243, Apr. 1966.

9. Loken, M. K., and Bugby, R. D.: Visualization of the lung by methods of scintiphotography, Amer. J. Roentgen., 97:850, Aug. 1966.

10. Morgan, R. H.: Visual perception in fluoroscopy and radiography, Radiology, 86:403, Mar. 1966.

11. Powell, M. R., and Anger, H. O.: Triple isotope renal evaluation with the scintillation camera, J. Nucl. Med., 7:373, May 1966. (Abstr.)

12. Powell, M. R., and Anger, H. O.: Blood flow visualization with the scintillation camera, J. Nucl. Med., 7:729, Oct. 1966.

13. Tuddenham, W. J.: Visual search, image organization, and reader error in roentgen diagnosis. Studies of the psychophysiology of roentgen image perception, Radiology, 78:694, May 1962.